Supporting Information

Vacuum dried flexible hydrophobic aerogels using bridged methylsiloxane as reinforcement : performance regulation with alkylorthosilicate or alkyltrimethoxysilane co-precursors

Dangjia Chen,[a] Keyi Dong,[b] Hongyi Gao,*[a] Tao Zhuang,[a] Xiubing Huang[a] and Ge Wang*[a]

[a] Beijing Advanced Innovation Center for Materials Genome Engineering, Beijing Key Laboratory of Function Materials for Molecule & Structure Construction, School of Materials Science and Engineering, University of Science and Technology Beijing, Beijing 100083, PR China.

[b] Beijing National Day School, Beijing 100039, PR China.

*Corresponding author at: No. 30, Xueyuan Road, Haidian District, Beijing City, PR China.

*E-mail: gewang@mater.ustb.edu.cn. (G. Wang)

*E-mail: hygao2009@163.com (H. Y. Gao)

Table S1. The detailed formulas of the products.

sample	APDEMS (mmol)	TPAL (mmol)	TMOS (mmol)	TEOS (mmol)	MTMS (mmol)	PTMS (mmol)	HTMS (mmol)	EtOH (ml)	Water (ml)
DT	12.81	6.39	0	0	0	0	0	18	2
DT-Q-M	4.27	2.13	8.54	0	0	0	0	18	2
DT-Q-E	4.27	2.13	0	8.54	0	0	0	18	2
DT-T-M	4.27	2.13	0	0	8.54	0	0	18	2
DT-T-P	4.27	2.13	0	0	0	8.54	0	18	2
DT-T-H	4.27	2.13	0	0	0	0	8.54	18	2

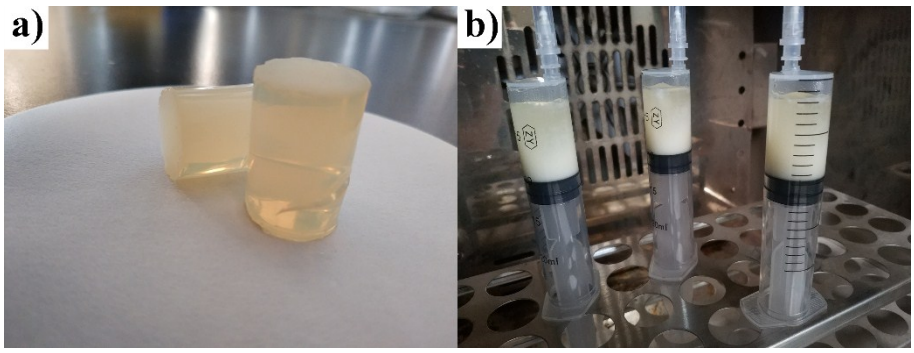

Figure S1. DT-Q-M in drying process (a), DT-T-H in sol-gel process (b).

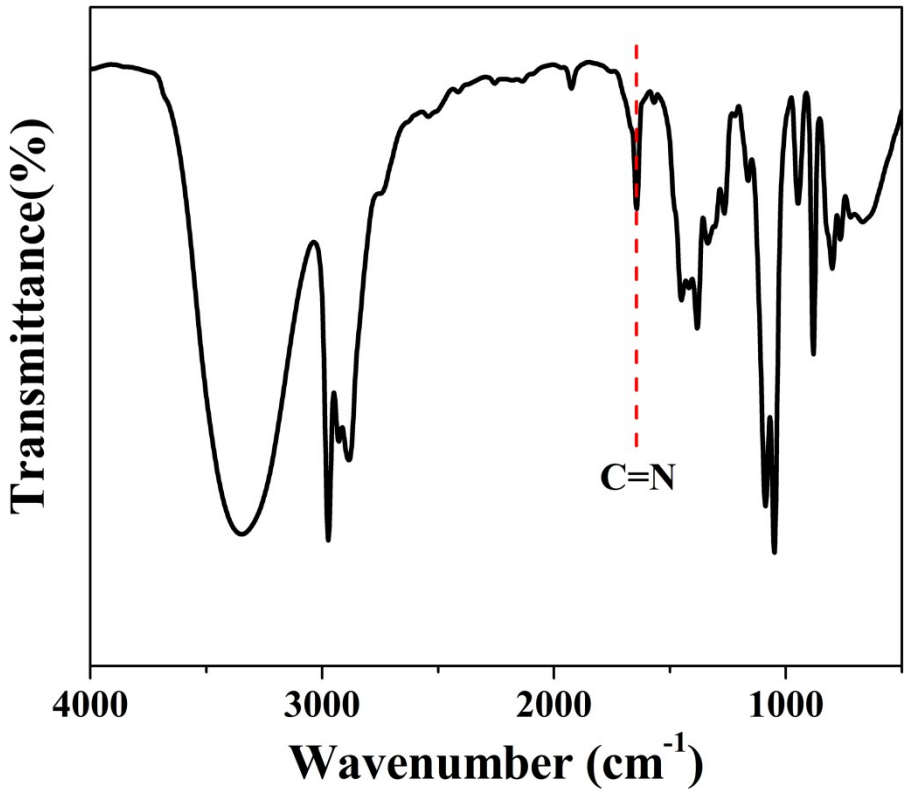

Figure S2. The FT-IR spectrum of the BMSQ precursor, in the synthesis of the aerogel, the mixture of ethanol, TPAL and ATDEMS was measured by the FT-IR before water was added, the generation of the imine and the disappearance of the aldehyde group means the precursor was synthesized.

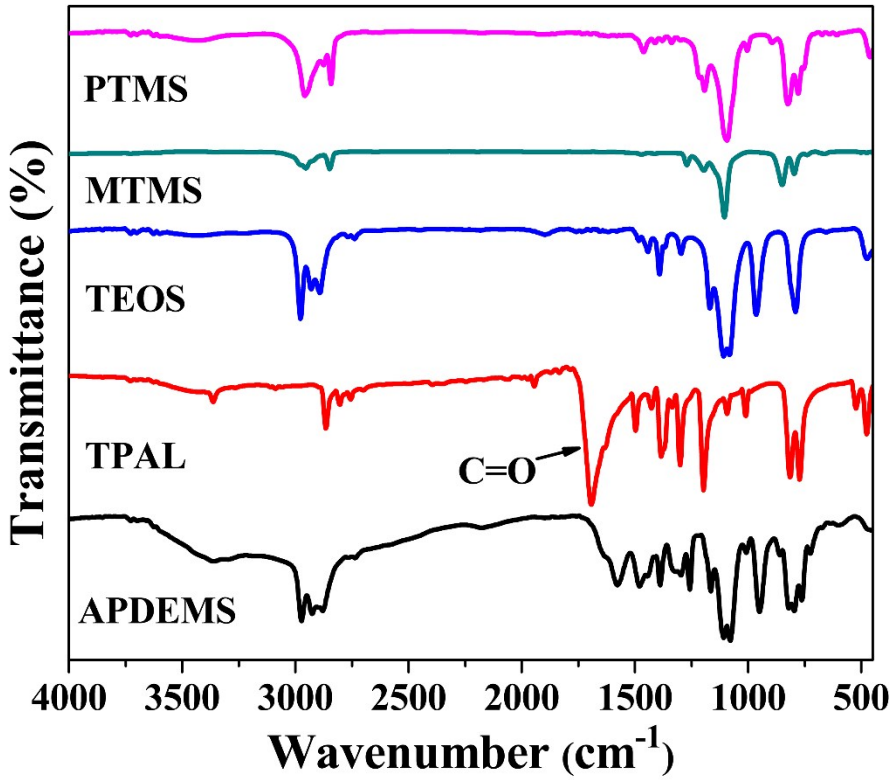

Figure S3. The FT-IR spectra of the start monomers.

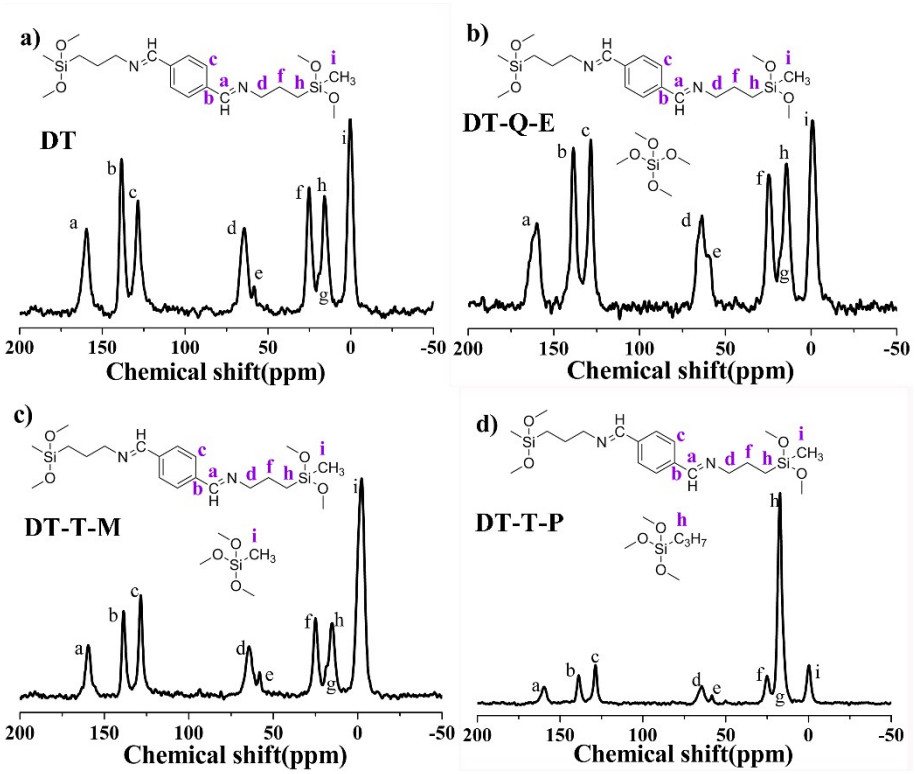

Figure S4. The Solid-state ^{13}C NMR spectra of the aerogels.

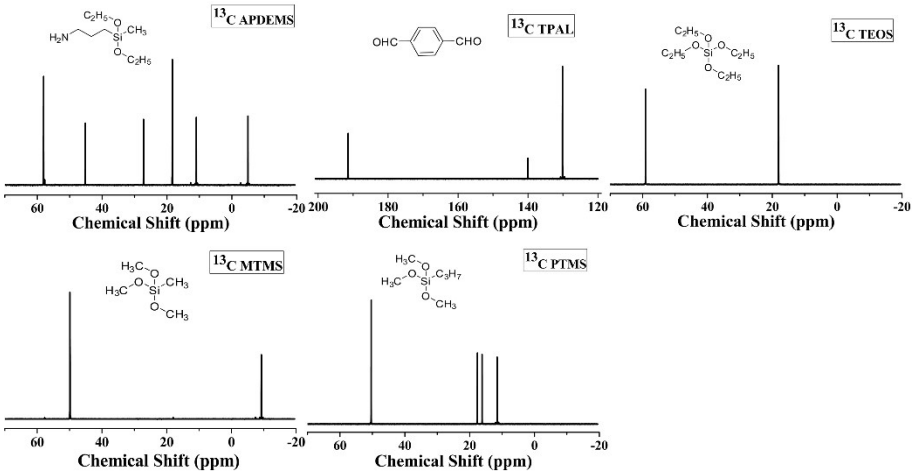

Figure S5. The ^{13}C NMR spectra of the start monomers.

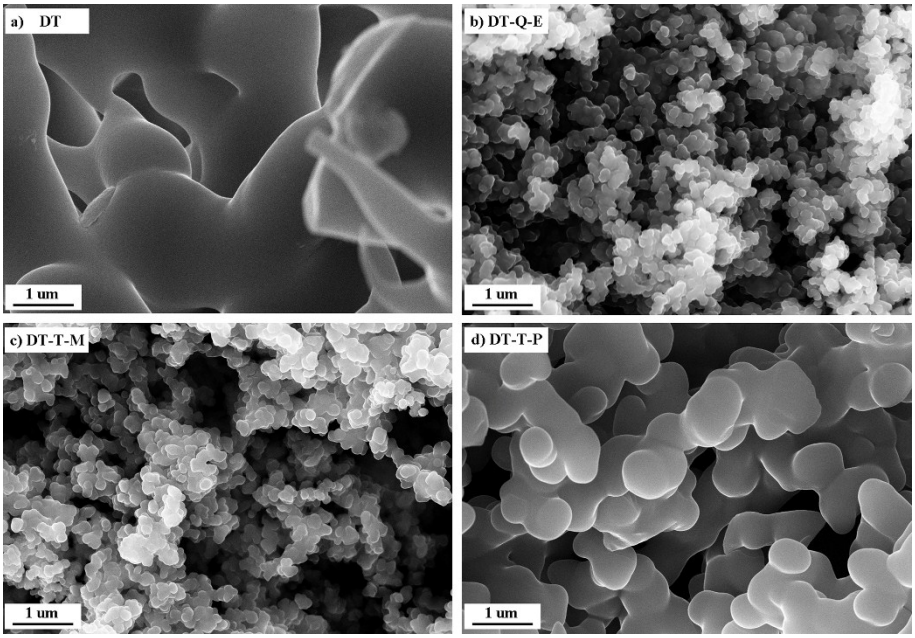

Figure S6. The SEM images of the aerogels with 40000 times magnification.

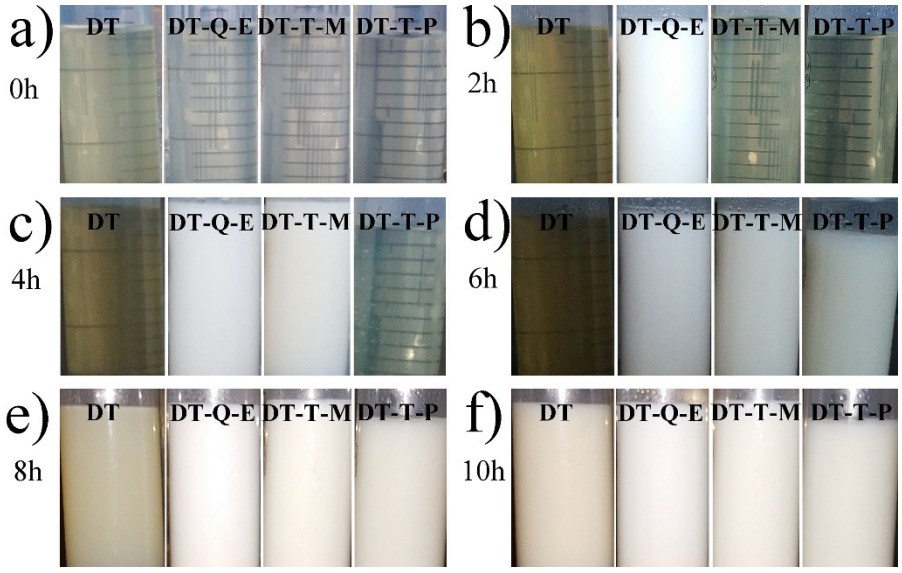

Figure S7. Photos of the sol-gel process of the samples in every 2 hours.

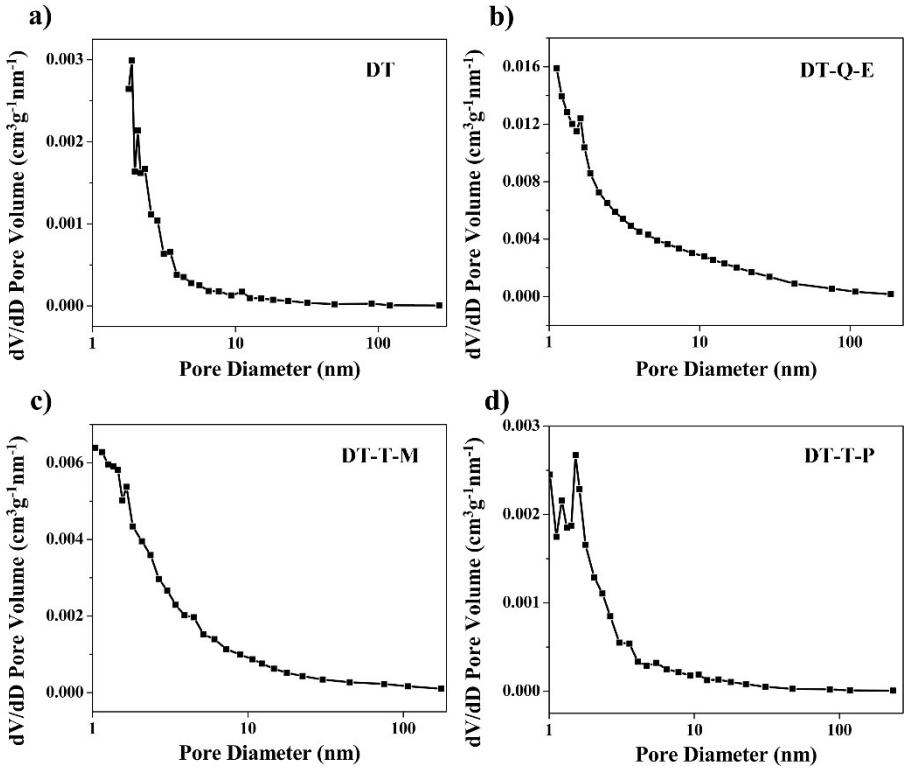

Figure S8. Pore size distribution of the aerogels, a) DT, b) DT-Q-E, c) DT-T-M, d) DT-T-P.

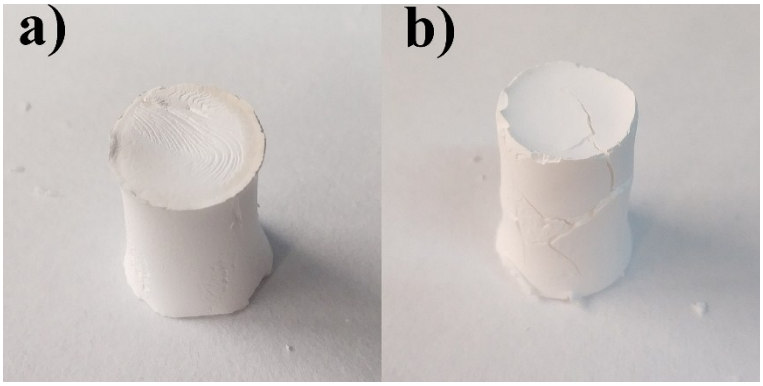

Figure S9. The optical images of aerogels, a) DT-T-3M, b) DT-Q-3E.

To improve the specific surface areas, the content of MTMS and TEOS was increased by 3 times as the content in DT-T-M and DT-Q-E individually, the two kind aerogels were named DT-T-3M and DT-Q-3E. DT-T-3M and DT-Q-3E both suffered larger shrinkage and even fragmentation, the specific surface area of DT-T-3M and DT-Q-3E are 69.88 and 265.41 m^2/g, and the shrinkage of DT-T-3M and DT-Q-3E are 33.7% and 27.9% individually.

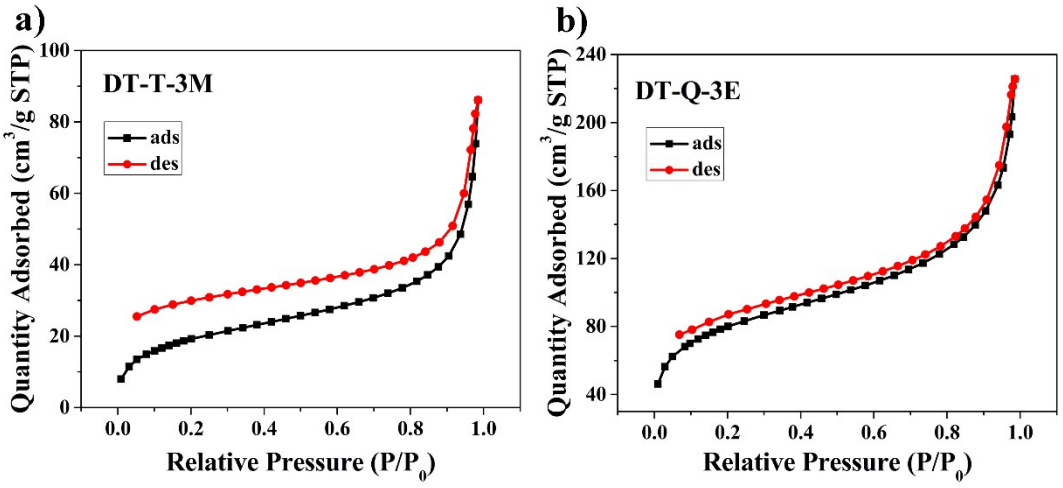

Figure S10. The Nitrogen adsorption and desorption isotherms of a) DT-T-3M and b) DT-Q-3E.

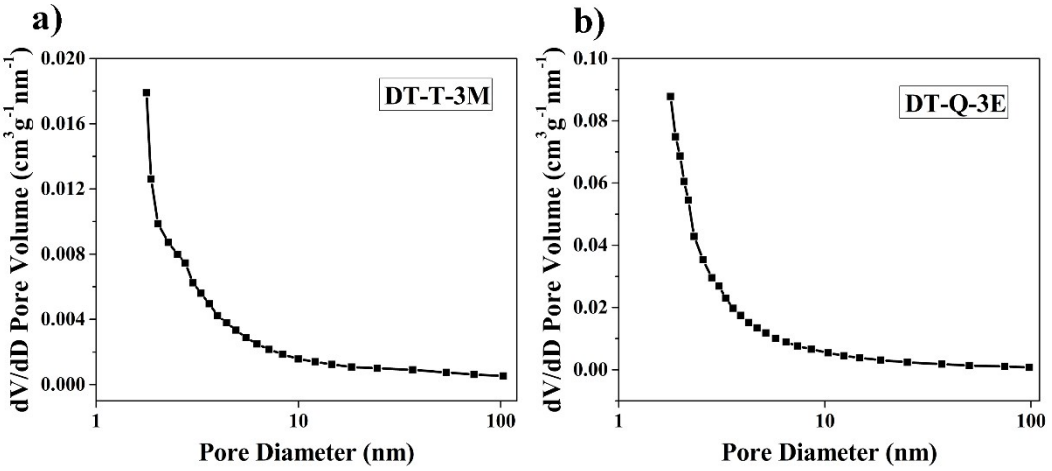

Figure S11. Pore size distribution of the aerogels, a) DT-T-3M, b) DT-Q-3E.

Table R1. A comparison of the removal rate and separation efficiency of aerogel in this work and the rate of materials reported in previous works.

Material	Removal rate ($L \cdot m^{-2} \cdot s^{-1}$)	Separation efficiency	Reference
mesh	20	93%	1
mesh	15	96%	2
membrane	0.13	99%	3
membrane	0.09	100%	4
Aerogel (monolith)	0.18	99%	This work

Reference 1: J. Li, L. Yan, H. Li, J. Li, F. Zha and Z. Lei, RSC Adv., 2015, 5, 53802;
Reference 2: J. Li, L. Yan, H. Li, W. Li, F. Zha and Z. Lei, J. Mater. Chem. A, 2015, 3, 14696;
Reference 3: X. Gao, L. Xu, Z. Xue, L. Feng, J. Peng, Y. Wen, S. Wang, and X. Zhang, Adv. Mater., 2014, 26, 1771;
Reference 4: M. Obaid, N. A. M. Barakat, O.A. Fadali, M. Motlak, A. A. Almajid and

K. A. Khalil, Chem. Eng. J., 2015, 259, 449.